Dielectrons in water clusters

Harri-Pekka Kaukonen[a], R. N. Barnett, and Uzi Landman
School of Physics, Georgia Institute of Technology, Atlanta, Georgia 30332

(Received 13 January 1992; accepted 27 March 1992)

The energetics, structure, and stability of a dielectron solvated in an internal cavity in water clusters, $(H_2O)_n^{-2}$, at 300 K are investigated using coupled quantum-classical molecular-dynamics simulations. In these calculations the ground state of the dielectron is calculated concurrently with the atomic configurations using the local-spin-density functional method, and the nuclear degrees of freedom evolve classically on the Born–Oppenheimer potential-energy surface. For $n = 64$ and 128 the internal single-cavity dielectron state is unstable, while for $n = 256$ (as well as in bulk water) it is energetically stable, fluctuating between a compact spherical configuration (e_{2c}) and an elongated ellipsoidal dumbbell-shaped one (e_{2d}). Transitions between these two states of the dielectron are accompanied by structural and orientational transformations of the surrounding water molecules. The induced molecular orientational order is enhanced and is of longer range in $(H_2O)_{256}^{-2}$ than is the case for a solvated single excess electron. By extrapolating our results to the bulk limit we conclude that a spin-paired dielectron state in bulk water, at 300 K, is a stable species relative to two single separated hydrated electrons.

I. INTRODUCTION

Investigations of electron solvation phenomena in bulk liquid water[1] and ammonia[2] are perhaps the earliest investigations of electronic states in liquids.[3] More recently, experimental and theoretical developments[4] revealed a wealth of information pertaining to localization modes,[3,4] energetics,[3,4] structure,[3,4(a),4(c)] solvation dynamics,[5] and spectra[6] of excess electrons in finite water clusters of variable size, as well as in bulk aqueous media.[7-9]

While states of two electrons (dielectrons—e_2) trapped in a single anion vacancy in ionic crystals[10] (F' centers) as well as in molten alkali-halide[11] and recently alkali-halide clusters,[12] and in disordered solids and liquids[13] are well known, the existence of e_2 in polar molecular liquids (water in particular) has been a subject of much debate.[13,14]

In this paper we explore the ground-state properties of spin-paired electrons (i.e., ^1S state) localized in liquid water clusters, suggesting an energetic stability of a dielectron state in sufficiently large clusters (i.e., $(H_2O)_n^{-2}$ for $n \gtrsim 250$) and in the bulk aqueous medium. The energetics, structure and dynamical properties of the e_2 state which we studied, using modern simulation methods, are likely to be of relevance to investigations of the microscopic mechanisms of certain chemical and physical consequences of radiological processes in water, although the expected reactivity of the species may complicate direct experimental probing of its properties.

A brief description of the simulation methods and a discussion of the electron–water pseudopotential used in the calculations are given in Sec. II. Our results for dielectrons in water clusters are exhibited and discussed in Sec. III. A summary of our findings is given in Sec. IV.

II. METHOD AND INTERACTION POTENTIALS

In our molecular-dynamics simulations the intra- and intermolecular interactions in water are described by the RWK2-M potentials,[15] [equilibrium averaged results for neutral clusters $(H_2O)_n$, $n = 64$, 128, and 256 are given in Appendix A], and the interactions with the excess electrons are given by model pseudopotentials.[3(a)] The configurational space of the coupled classical (water)–quantum (electrons) system is explored on the Born–Oppenheimer (BO) potential surface, with the ground-state electronic structure of the excess electrons evaluated (concurrent with the instantaneous water molecules' nuclear configurations) via the local-spin-density (LSD) functional method; details of the method of self-consistent solution of the LSD Kohn–Sham equations and the exchange-correlation functional used by us can be found elsewhere[12,16] [in this context we remark that in all our calculations the spatial grids employed were chosen to assure convergence; typically, spatial grids of $(32\times32\times32)$ points with a grid spacing of 1 a.u. were used]. In calculations involving a single excess electron both the BO-LSD and ground-state dynamics (GSD)[4(c),5(b)] methods were used, yielding very similar results.

Prior to presentation of our results, we comment on the nature of the pseudopotentials describing the electron–water molecule interactions. In our earlier investigations of the solvation of single excess electrons in water clusters of variable sizes, we have constructed and employed[3] a pseudopotential (V) consisting of additive contributions from Coulomb interactions with the molecular point changes (V_c); exchange ($V_x \propto -\alpha_x \rho^{1/3}$, where ρ is the electronic charge distribution of the ground-state water molecule, and $\alpha_x = 0.3$ was determined by fitting the binding energy in $(H_2O)_8^{-1}$ to quantum-chemical calculations); exclusion ($V_e \propto \rho^{2/3}$, which accounts for orthogonalization of the excess electron wave function to the molecular electronic wave functions,

[a] Permanent address: Laboratory of Physics, Helsinki University of Technology, 02150 Espoo, Finland.

 0021-9606/92/141365-13$06.00

i.e., Pauli exclusion); and a polarization potential $[V_p(\mathbf{r},\mathbf{R}_0) = -0.5\alpha_{op}e^2/(|\mathbf{r}-\mathbf{R}_0|^2 + R_p^2)^2$, where $\mathbf{r}$ and $\mathbf{R}_0$ are the vector positions of the excess electron and molecular oxygen, respectively, α_{op} is the isolated water molecule spherically averaged electronic (optical) polarizability, and R_p was determined by fitting to a calculated adiabatic polarizability potential of water[3(a)]. The excess electron vertical binding energies calculated with the above pseudopotential were found[3(b),4(c)] to be in good agreement with those available at the time from photoelectron measurements[17] for $(H_2O)_n^-$ ($n \leqslant 18$), and have led to the prediction of surface and internal localization modes in water clusters,[3,4(a),4(c)] the evolution of spectral characteristics with size,[6] and subpicosecond dynamics of the solvation process.[5] Furthermore, these studies led to the formulation of a dielectric continuum model of finite clusters[3(b),18] with the vertical binding energy (VBE) of an excess electron localized in an internal state in a cluster of mean radius $\overline{R} = r_s n^{1/3}$, where r_s is the mean radius of a water molecule and n the number of molecules in the cluster, given by

$$\begin{aligned} \mathrm{VBE}(\overline{R}) &= \mathrm{VBE}(\infty) + A\overline{R}^{-1} \\ &= \mathrm{VBE}(\infty) + (A/r_s)n^{-1/3}, \end{aligned} \tag{1}$$

where

$$A = \frac{e^2}{2}\left(1 + \frac{1}{\epsilon_{op}} - \frac{2}{\epsilon_s}\right),$$

and ϵ_{op} (ϵ_s) are the optical (static) dielectric functions, and $\mathrm{VBE}(\infty)$ the value in the bulk, i.e., the value obtained when $n \to \infty$ (a similar expression was given for the adiabatic binding energy [$\mathrm{ABE}(\overline{R})$] with $\mathrm{ABE}(\infty)$ and $A = (e^2/2)(1 - 1/\epsilon_s)$ replacing the corresponding terms in Eq. (1)).

In the course of our studies, coupled with the more recent availability[4(b)] of photoelectron data for $(H_2O)_n^-$ clusters with $n \leqslant 70$, a tendency in the calculations toward overbinding of the excess electron in large clusters was noted. Consequently, we reexamined our model assumptions, and in particular the compatibility with the continuum dielectric theory which is expected to apply best at the large cluster-size regime.[3(b),18] Since in our model the molecular electronic charge distribution is nonpolarizable (i.e., the dielectric constant $\epsilon = \epsilon_{or}$ and $\epsilon_{op} = 1$, where ϵ_{or} is the orientational dielectric function, and for water $\epsilon_s \approx \epsilon_{or}$), the correspondence of the vertical binding energy in the microscopic simulations with the dielectric continuum sphere expression [Eq. (1)] may be expressed as

$$\mathrm{VBE}'(\overline{R}) = \mathrm{VBE}'(\infty) + A'\overline{R}^{-1} + 2\pi\rho_m\alpha_{op}e^2/\overline{R}, \tag{2}$$

where $A' = e^2(1 - 1/\epsilon_{or})$ and the term containing the molecular density (ρ_m) and the optical polarizability α_{op} of the water molecule, accounting for the induced electronic polarization of the medium (corresponding to the term V_p in the model pseudopotential). However, the aforementioned leads to an inconsistency with Eq. (1) since Eq. (2) can be obtained from Eq. (1) by replacing the term $1/\epsilon_{op}$ by $1 + 4\pi\rho_m\alpha_{op}$, but $1/\epsilon_{op} < 1$. Furthermore, we note that assuming $\alpha = \alpha_{op} + \alpha_{or}$, where α_{or} is the orientational polarizability of the aqueous medium, and thus $\epsilon_s = 1 + 4\pi\rho_m(\alpha_{op} + \alpha_{or})$ and $\epsilon_{op} = 1 + 4\pi\rho_m\alpha_{op}$, and for $\alpha_{or} \gg \alpha_{op}$, which is the case for water, leads from Eq. (1) to

$$\mathrm{VBE}''(\overline{R}) = \mathrm{VBE}''(\infty) + A''\overline{R}^{-1} - 2\pi\rho_m\alpha_{op}e^2/\overline{R}, \tag{3}$$

where $A'' = e^2(1 - 1/\epsilon_{op})$. Therefore, it appears that short of a reformulation to include electronically polarizable water molecules, it is advisable, for the large cluster regime, to not include the V_p term in the electron–water pseudopotential, V, and reparametrize V (i.e., fit α_x in the short-range exchange term) in such a manner as to adequately reproduce the results for the small cluster-size regime,[3(b)] while maintaining consistency with the continuum dielectric expression [i.e., Eq. (1) with $\epsilon_{op} = 1$]. Following this procedure yields $\alpha_x = 0.57$, with the excess electron in $(H_2O)_n^-$ bound as a surface state for $n \leqslant 32$, gradually converting into an internally solvated electron for larger clusters, exhibiting structural (i.e., spatial extent of the excess electron distribution, molecular solvation shell structure, and molecular preferential orientational ordering in the near-solvation shells) and spectral properties similar to those found by us previously but with corresponding energetic characteristics (i.e., VBE's) in closer agreement with recent[4(b)] experimental data (see Appendix B).

In light of the above discussion most of the results which we present for dielectron systems in the following section correspond to calculations using the modified potential [energetic results for $(H_2O)_{256}^{-2}$ using the original pseudopotential are given for comparison in Appendix C].

III. DIELECTRONS IN WATER

A. Energetics and stability

Two electrons may localize in a cluster in various configurations including both electrons localized in the same internal solvation cavity, the two electrons localized in two separate internal solvation cavities, both electrons bound in surface states, and one electron bound internally and the other localized at the surface. Additionally, at finite temperature the system may fluctuate among several of the aforementioned configurations. In this study we focus on the first possibility, i.e., the energetics and structure of an electron pair localized in a single solvation cavity. In addition to its analogy to the F' center in ionic salts, this localization mode may constitute a precursor for certain two-electron reactions in water.

Therefore, in most of our studies, we started our dielectron simulations [i.e., $(H_2O)_n^{-2}$] from a corresponding equilibrated internally localized single-electron configuration [i.e., $(H_2O)_n^-$]. In all cases the simulations were performed at 300 K (i.e., canonical simulations) with the temperature controlled via infrequent stochastic thermalization of the classical (molecular) degrees of freedom.[3,4(a),4(c)] In addition, since our purpose in this study is to investigate the equilibrium properties of the system (which are independent of the masses of the classical constituents), the dynamical evolution of the classical degrees of freedom was performed

in some of our calculations with the mass of the oxygen atoms taken the same as that of the hydrogens, which enhances the effectiveness of exploration of the available phase space of the system. The time step used in the molecular-dynamics simulations of the classical degrees of freedom was $\Delta t = 0.25$ fs.

Prior to presenting our results we introduce the notation that will be used throughout our discussion.

(i) Quantities corresponding to a single excess electron in a cluster containing n water molecules are denoted by a subscript "1," e.g., $\mathrm{VBE}_1^{(n)}$, $\mathrm{ABE}_1^{(n)}$, and $E_{C1}^{(n)}$ are the vertical, adiabatic, and molecular reorganization energies of a cluster $(H_2O)_n^{-1}$, respectively. The corresponding quantities for a cluster containing an excess dielectron are denoted by a subscript "2" (e.g., $\mathrm{VBE}_2^{(n)}$, $\mathrm{ABE}_2^{(n)}$, and $E_{c2}^{(n)}$).

When reference is made to excess electron states in bulk water a superscript "∞" is used, e.g., VBE_q^{∞} and ABE_q^{∞} refer to the vertical and adiabatic binding energies of an excess single ($q = 1$) or dielectron ($q = 2$) in bulk water, respectively.

In this context we note that the cluster reorganization energy $E_{cq}^{(n)} = \langle\phi\rangle_{(H_2O)_n^{-q}} - \langle\phi\rangle_{(H_2O)_n}$ ($q = 1$ or 2) is the difference between the equilibrium intra- and intermolecular interaction potential energies of the solvent cluster, with and without the solvated electron(s). The adiabatic binding energy of the excess electron(s) in the cluster is given by $\mathrm{ABE}_q^{(n)} = \mathrm{VBE}_q^{(n)} + E_{cq}^{(n)}$ (for a bound state $\mathrm{VBE}_q^{(n)} < 0$ and $E_{cq}^{(n)} > 0$, thus $\mathrm{ABE}_q^{(n)} > \mathrm{VBE}_q^{(n)}$).

(ii) A system in its equilibrium state with respect to the molecular constituents is denoted as $(H_2O)_n^{-q}$, with $q = 1$ or 2 corresponding to a hydrated single electron or dielectron, respectively. A state of a system (neutral or charged) reached via a *vertical* transition from an initial equilibrium system, i.e., where the molecular configuration in the final state is not relaxed but is kept as that corresponding to the initial state, is denoted by $[(H_2O)_n^{-q+1}]_q$. Thus a *vertical transition* from the equilibrium state of a dielectron in a water cluster of size n to the neutral corresponds to $(H_2O)_n^{-2} \rightarrow [(H_2O)_n]_2 + 2e^-$ and the vertical ionization potential (VIP), i.e., the energy required to remove the two excess electrons in a vertical process, is $\mathrm{VIP}_{2\rightarrow 0} = -\mathrm{VBE}_2^{(n)}$.

Similarly, the *vertical removal* of one of the electrons from the initially equilibrated dielectron state, i.e., $(H_2O)_n^{-2} \rightarrow [(H_2O)_n^{-1}]_2 + e^-$, requires an energy $\mathrm{VIP}_{2\rightarrow 1}^{(n)}$, while the *adiabatic* single-electron ionization of an equilibrated dielectron system, i.e., $(H_2O)_n^{-2} \rightarrow (H_2O)_n^{-1} + e^-$, requires an energy $\mathrm{AIP}_{2\rightarrow 1}^{(n)} = \mathrm{ABE}_2^{(n)} - \mathrm{ABE}_1^{(n)}$ (or $\mathrm{AIP}_{2\rightarrow 1}^{(n)} = \mathrm{VBE}_2^{(n)} - \mathrm{VBE}_1^{(n)} + E_{c2}^{(n)} - E_{c1}^{(n)}$).

The first issue which we need to explore is the cluster-size range for stable dielectron localization. In simulation studies stability may be assessed in several ways: (i) The most elementary argument is that concerning the lack of stability which would express itself in the inability to form the required state in the first place, or in a "transient nature" of the state. (ii) Another stability criterion of a solvated species involves the sign (and magnitude) of the adiabatic binding energy, with $\mathrm{ABE}_q^{(n)} < 0$ corresponding to a stable state and the reverse for $\mathrm{ABE}_q^{(n)} > 0$.

An additional stability criterion (iii) for dielectron solvation may be expressed as [this criterion is used in Ref. 13 with the opposite sign to that in Eq. (4)]

$$\Delta_n(d) = \tfrac{1}{2}\mathrm{ABE}_2^{(n)} - \mathrm{ABE}_1^{(n)}(d), \tag{4}$$

where $\mathrm{ABE}_q^{(n)}$ is the adiabatic binding energy for solvation of an excess single electron ($q = 1$) or dielectron ($q = 2$) in a system of size n, with d the distance between the two single solvated electrons. Since we focus on e_2 states localized in the same solvation cavity, we do not use Eq. (4) in our study of clusters. However, the above criterion becomes useful (with $d \rightarrow \infty$ and $n \rightarrow \infty$) when we extrapolate our results to dielectrons in bulk liquid water (see below).

Our attempts to localize a stable dielectron in $(H_2O)_n^{-2}$ clusters, with $n = 64$ and 128 indicated that in this cluster-size range a dielectron state bound in the same cavity is metastable at best. Thus, for the $n = 64$ cluster an initial e_2 state "decomposed," after about 2500 integration steps, with one of the electrons expelled from the cluster interior [see Fig. 1(b)], and for $n = 128$ a long-lived metastable state formed with $\mathrm{VBE}_2^{(128)} = (-0.214 \pm 0.023)$ a.u., $E_{c2}^{(128)} = 0.22$ a.u., and $\mathrm{ABE}_2^{(128)} = 0.006$ a.u.

Subsequently, we investigated same-cavity-localized e_2 states in a larger cluster, i.e., $(H_2O)_{256}^{-2}$. The energetics of the cluster is summarized in Table I and in Fig. 2 (since in the following our discussion focuses on the properties of this

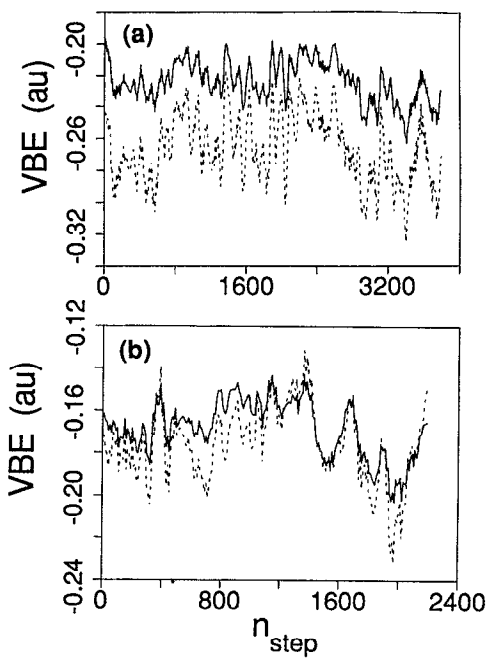

FIG. 1. (a) Vertical binding energy (VBE) of a dielectron (dashed line) and of a single electron (solid line), with the water molecules maintained as those of the dielectron cluster, for $(H_2O)_{256}$ at 300 K, vs the number of integration steps in a segment of the simulation. (b) Same as in (a) but for $(H_2O)_{64}$. The simulation started with the dielectron localized internally in the cluster. At the end ($n_{\mathrm{step}} > 2000$) the cavity-bound dielectron unbinds and one of the electrons is expelled (delocalized) indicating an instability of the dielectron in $(H_2O)_{64}$. Energy in a.u. units (1 a.u. = 27.21 eV).

TABLE I. Energetics, calculated via BO-LSD simulations using the modified electron–water pseudopotential, of a dielectron internally localized in $(H_2O)_{256}^{-2}$ at 300 K. $\langle\phi_1\rangle_2$, $\langle\phi_2\rangle_2$, and $\langle\phi\rangle_2$ are the intra-, inter-, and total potential energies of the water molecules. $\langle V\rangle_2$, $\langle K\rangle_2$, $\langle E_{xc}\rangle_2$, and $\langle E_H\rangle_2$ are the contributions of the electron–water interaction, electronic kinetic energy, exchange-correlation term, and Hartree energy, respectively, to the total dielectron energy. VBE_2 is the vertical binding energy of the dielectron (i.e., sum of the aforementioned contribuitons); E_{c2} is the cluster molecular reorganization energy for the dielectron, and ABE_2 is the dielectron adiabatic binding energy. The reorganization energy associated with the process $(H_2O)_{256}^{-2} \rightarrow (H_2O)_{256}^{-1} + e^-$ is given by $E_{c2\rightarrow 1} = \langle\phi\rangle_2 - \langle\phi\rangle_1$ ($\langle\phi\rangle_1$ is given in Table III). Results for the compact, dumbbell-shaped, and intermediate dielectron states (e_{2c}, e_{2d}, and e_{2i}, respectively) were averaged over $5.8\times10^3\Delta t$, $3.3\times10^3\Delta t$, and $1.3\times10^3\Delta t$, respectively. The average properties of the dielectron are given in the first row. Uncertainty estimates are given in square brackets, and energies in a.u. units (1 a.u. = 27.21 eV).

	$\langle\phi_1\rangle_2$	$\langle\phi_2\rangle_2$	$\langle\phi\rangle_2$	$\langle V\rangle_2$	$\langle K\rangle_2$	$\langle E_{xc}\rangle_2$	$\langle E_H\rangle_2$	E_{c2}	VBE_2	ABE_2	$E_{c2\rightarrow1}$
average	0.6159	−3.9812	−3.3653 [0.030]	−0.5892	0.1539	−0.2357	0.3957	0.2179	−0.2754 [0.0244]	−0.0575	0.1415
e_{2c}	0.6194	−3.9768	−3.3574	−0.6042	0.1490	−0.2349	0.4066	0.2258	−0.2834 [0.0239]	−0.0576	0.1494
e_{2d}	0.6100	−3.9865	−3.3764	−0.5647	0.1632	−0.2385	0.3773	0.2068	−0.2627 [0.0213]	−0.0559	0.1304
e_{2i}	0.6153	−3.9883	−3.3730	−0.5839	0.1521	−0.2323	0.3930	0.2102	−0.2710 [0.0184]	−0.0608	0.1338

cluster the superscript denoting the size of the cluster is omitted). The energetics of the dielectron in $(H_2O)_{256}^{-2}$, using the unmodified potential, given in Appendix C, shows similar characteristics to those calculated with the modified electron–molecule pseudopotential, but exhibiting stronger binding.

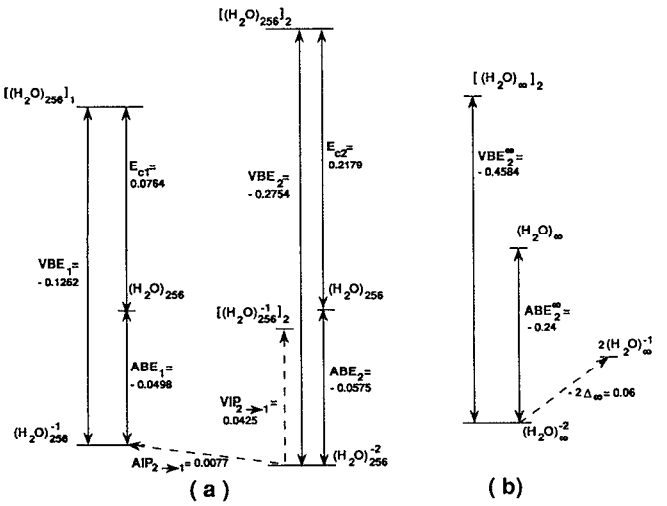

FIG. 2. Schematic diagrams of the energetics of hydration in a cluster containing 256 water molecules (a) and in bulk water (b). States of the cluster which are equilibrated with respect to the molecular constituents are denoted by $(H_2O)_{256}^{-q}$, $q = 2$, 1, and 0, corresponding to a hydrated dielectron, single electron, and neutral cluster, respectively. Final states resulting from a vertical ionization process in which m electrons are removed ($m = 1$ or 2) are denoted by $[(H_2O)_{256}^{-q+m}]_q$, where $q = 2$ or 1 is the charge state of the initial state, and the square brackets denote that the electronic final state is calculated in the molecular geometry of the initial state of excess charge q. VBE_q and ABE_q are the vertical and adiabatic binding energies of the excess hydrated species ($q = 2$ corresponding to a dielectron), respectively, and E_{cq} is the corresponding cluster molecular reorganization energy. The dashed lines denote vertical and adiabatic ionization potentials of the process connected by line. For the bulk system (b) the number of molecules (256) in the above notations is replaced by the symbol ∞. The dashed line in (b) corresponds to the dissociation process $(e_2)_{hyd} \rightarrow 2(e_1)_{hyd}$ of a dielectron into two separated hydrated single electrons, with the dissociation energy given by $-2\Delta_\infty$ [see Eq. (4)]. Another method of estimation, based on the continuum dielectric model yields $ABE_2^\infty = -0.15$ a.u. and $-2\Delta_\infty = 0.03$ a.u. Energies are in a.u. units (1 a.u. = 27.21 eV).

From Table I we observe first that the time-averaged adiabatic binding energy of $(H_2O)_{256}^{-2}$ with reference to the neutral cluster indicates a stable e_2 state [i.e., $ABE_2 = -0.0575$ a.u., see criterion (ii)]. In addition $ABE_2 < ABE_1$ ($AIP_{2\rightarrow1} = 0.0077$ a.u. = 0.21 eV, using the value of $ABE_1 = -0.0498$ a.u. from Table III) indicating stability of the dielectron cluster also with respect to a single solvated excess electron [i.e., $(H_2O)_{256}^{-1} + e^-$]. Furthermore, in Fig. 1(a) we show the time variation of VBE_2 in $(H_2O)_{256}^{-2}$ (dashed line) as well as the binding energy of a single excess electron calculated for the same molecular configurations of the doubly charged cluster. As seen, the dielectron is more bound (i.e., larger magnitude of VBE_2) than the single electron, with the water molecular configurations maintained as those of the dielectron cluster (this behavior remains the same throughout all our simulations of the cluster). In contrast to the above, the corresponding binding-energy data shown in Fig. 1(b) for the $(H_2O)_{64}^{-2}$ cluster, recorded up to the point of "decomposition" of the dielectron state, indicate only marginal transient preference for the two electrons to be localized in the internal cavity, with an eventual terminal reversal ($n_{step} \sim 2200$) in the relative magnitudes of the energies, which coincides with delocalization and unbinding of the e_2 state.

To estimate the binding energies and stability of a dielectron localized in a cavity in bulk water at 300 K we show in Fig. 3 a plot vs r^{-1} of $\int_0^r \langle V(r')\rangle 4\pi r'^2 dr'$ (i.e., the interaction energy between the electrons and the water molecules integrated in a sphere of radius r about the centroid of the dielectron distribution). The asymptotic value at $r^{-1} \rightarrow 0$, denoted by $\langle V\rangle_\infty = -0.7722$ a.u., corresponds to the bulk limit. Since for the $(H_2O)_{256}^{-2}$ cluster we may assume that the Hartree ($\langle E_H\rangle_2$), exchange-correlation ($\langle E_{xc}\rangle_2$), and electronic kinetic energy ($\langle K\rangle_2$) contributions have saturated [i.e., achieved their bulk limit; an assumption supported by comparison of these quantities with those corresponding to $(H_2O)_{128}^{-2}$], the vertical binding energy of a single-cavity-localized dielectron in bulk water can be estimated to be

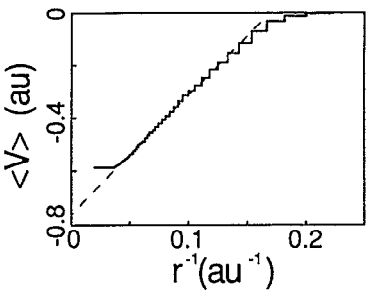

FIG. 3. Electron–water interaction $\langle V \rangle$ integrated over a sphere of radius r about the centroid of the dielectron distribution localized internally in $(H_2O)_{256}^{-2}$ at 300 K, plotted vs r^{-1}. Energy in a.u., and distance in units of inverse Bohr radii (a.u.$^{-1} = a_0^{-1}$).

$\mathrm{VBE}_2^{\infty} = \langle V \rangle_{\infty} + (\langle E_H \rangle_2 + \langle E_{xc} \rangle_2 + \langle K \rangle_2)$, yielding a value of -0.4584 a.u. (or -12.46 eV). In this context we note that a similar procedure for the single excess electron case, or alternatively from the asymptotic value of $\langle \mathrm{VBE} \rangle_1$ plotted vs $n^{-1/3}$ (see Fig. 14 in Appendix B), yields $\mathrm{VBE}_1^{\infty} = -0.17$ a.u., or -4.62 eV (note that in view of the computational error estimates shown in Fig. 14 this value may be regarded as an upper bound on the calculated magnitude). The adiabatic binding energy of the e_2 state in bulk water is estimated by $\mathrm{ABE}_2^{\infty} = \mathrm{VBE}_2^{\infty} + E_{c2}$ [where it is assumed that the reorganization energy achieved the bulk limit for the $(H_2O)_{256}^{-2}$ cluster], yielding $\mathrm{ABE}_2^{\infty} = -0.24$ a.u. (or -6.5 eV). The corresponding value for a single solvated electron (upper bound, on the magnitude, see Appendix B) is $\mathrm{ABE}_1^{\infty} = -0.09$ a.u. (or -2.4 eV). Application of criterion (iii), given in Eq. (4), yields $\Delta_{\infty} = -0.03$ a.u. (or -0.82 eV), indicating stability of the cavity-localized dielectron state in bulk water [$-2\Delta_{\infty} = 0.06$ a.u. is the adiabatic energy required to dissociate a dielectron in water into two separated solvated electrons, see Fig. 2(b)].

Another estimate of the stability of the cavity-localized dielectron state in bulk water, which avoids the assumption that the molecular reorganization energy achieved the bulk limit for the $(H_2O)_{256}^{-2}$ cluster, is based on the dielectric continuum model of finite clusters,[3(b),18] in conjunction with results of our simulations.

From Eq. (1) with $\epsilon_{op} = 1$, and the corresponding equation for the adiabatic energy, we obtain

$$\mathrm{ABE}_q^{\infty} = \mathrm{ABE}_q^{(n)} + \tfrac{1}{2}\left[\mathrm{VBE}_q^{\infty} - \mathrm{VBE}_q^{(n)}\right], \qquad (5)$$

where $q = 1$ or 2 for an excess single or dielectron, respectively.

Using in the above equation the values $\mathrm{ABE}_2^{(256)} = -0.575$ a.u. and $\mathrm{VBE}_2^{(256)} = -0.2754$ a.u. from Table I, and $\mathrm{VBE}_2^{\infty} = -0.4584$ a.u., yields $\mathrm{ABE}_2^{\infty} = -0.15$ a.u. (or -4.08 eV). A similar calculation for the single excess electron, with $\mathrm{ABE}_1^{(128)} = -0.0295$ a.u. and $\mathrm{VBE}_1^{(128)} = -0.1069$ a.u. from Table III in Appendix B, and $\mathrm{VBE}_1^{\infty} = -0.17$ a.u., yields $\mathrm{ABE}_1^{\infty} = -0.06$ a.u. (or -1.63 eV). Note that this value for the adiabatic binding energy of the single excess electron in bulk water is in close agreement with the experimentally estimated[19] heat of hydration of an electron in water, $\Delta H(e_{aq}^-) \approx -1.7$ eV. (The above value obtained by using the data for $n = 128$, approximates well the average for the three cluster sizes which we simulated, see Appendix B.)

Using Eq. (4), with the above values for ABE_1^{∞} and ABE_2^{∞}, yields for the adiabatic energy required to dissociate a dielectron in bulk water into two separate solvated electrons $-2\Delta_{\infty} = 0.03$ a.u. (or 0.83 eV). Both this estimate and the larger value, obtained by us above by assuming that the cluster reorganization energy achieved the bulk limit for $(H_2O)_{256}^{-2}$, indicate relative stability of the dielectron in bulk water.

An additional quantity of interest for the dielectron in bulk water, which can be estimated using the continuum dielectric model and the simulation results, is the vertical first ionization potential, $\mathrm{VIP}_{2\to1}^{\infty}$. Assuming spherical symmetry and uniform dielectric properties the following expression can be derived:[20]

$$\mathrm{VIP}_{2\to1}^{\infty} = \mathrm{VIP}_{2\to1}^{(n)} - \tfrac{1}{2}\left(\mathrm{VBE}_2^{\infty} - \mathrm{VBE}_2^{(n)}\right), \qquad (6)$$

where $\mathrm{VIP}_{2\to1}^{(n)}$ is the vertical first ionization potential for a cluster containing n water molecules, VBE_2^{∞} is the vertical binding energy of the dielectron in the bulk, and $\mathrm{VBE}_2^{(n)}$ is the one in the cluster.

Using the values obtained in our simulations for a dielectron in a 256-water molecule cluster (i.e., $\mathrm{VBE}_2^{(256)} = -0.2754$ a.u., see Table I, and $\mathrm{VIP}_{2\to1}^{(256)} = 0.0425$ a.u., see below), and $\mathrm{VBE}_2^{\infty} = -0.4584$ a.u., we obtain for the first vertical ionization potential of the dielectron in bulk water, $\mathrm{VIP}_{2\to1}^{\infty} = 0.134$ a.u. (or 3.65 eV). Related to this ionization potential is the energy required to vertically dissociate a dielectron into a single hydrated electron and one at the bottom of the water conduction band (which is estimated to be -1.1 eV below the vacuum level[4(b)]). Using the above value for $\mathrm{VIP}_{2\to1}^{\infty}$ we estimate this energy to be 2.55 eV.

Inspection of Table I reveals that the largest contribution to the electronic energy is from the overall attractive interaction with the water molecules ($\langle V \rangle_2$), with additional attraction coming from the exchange-correlation term ($\langle E_{xc} \rangle_2$). The main repulsive (positive) contribution originates from the Hartree (interelectronic repulsion) term ($\langle E_H \rangle_2$), with an added repulsive contribution from the electronic kinetic energy ($\langle K \rangle_2$) due to localization (confinement). Comparison of the dielectron results with those of a single excess electron [i.e., $(H_2O)_{256}^{-1}$, given in Appendix B] shows that the magnitude of $\langle V \rangle_2$ is more than twice that of $\langle V \rangle_1$, and the cluster molecular reorganization energy of the e_2 state (E_{c2}) is significantly larger than that for the single localized electron (E_{c1}). Finally, we note that the first vertical ionization potential of $(H_2O)_{256}^{-2}$, i.e., the energy associated with the process $(H_2O)_{256}^{-2} \to [(H_2O)_{256}^{-1}]_2 + e^-$ ($\mathrm{VIP}_{2\to1} = 0.0425$ [± 0.010] a.u., in Table I; see also Figs. 1 and 2) is significantly lower than that of $(H_2O)_{256}^{-1}$ ($\mathrm{VIP}_1 = -\mathrm{VBE}_1 = 0.1262$ a.u.; see Table III.). Similarly, the first adiabatic ionization energy of $(H_2O)_{256}^{-2}$ ($\mathrm{AIP}_{2\to1} = 0.0077$ a.u.) is lower than that for the singly charged cluster ($\mathrm{AIP}_1 = -\mathrm{ABE}_1 = 0.0498$ a.u.), and the adiabatic removal of one electron from the dielectron cluster is accompanied by a large reorganization energy (see $E_{c2\to1}$ in Table I).

B. Structure

Investigations of the electronic distribution and the molecular structures of the equilibrated dielectron $(H_2O)_{256}^-$ cluster reveal a most interesting behavior. As exhibited by the sample configurations shown in Figs. 4(a) and 4(b) the dielectron distribution fluctuates between an almost spherical compact state (which we will denote as e_{2c}) and an elongated ellipsoidal dumbbell-shaped state (denoted as e_{2d}). Contours in the xy plane of the electronic distributions for the e_{2c} and e_{2d} states are shown in Figs. 5 and 6(a), respectively, where for the latter contours of the spin-polarization function $p(\mathbf{r}) = \rho_\uparrow(\mathbf{r}) - \rho_\downarrow(\mathbf{r})$ are shown in Fig. 6(b) [$p(\mathbf{r})$ vanishes for the e_{2c} state]. In both states the dielectron is spin paired (^1S).

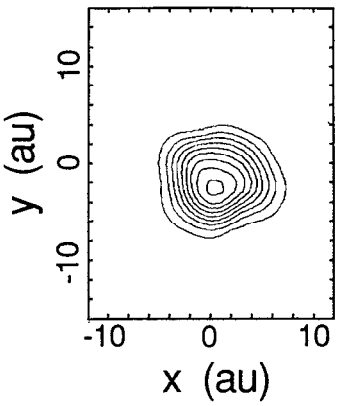

FIG. 5. Contours of electronic density for the e_{2c} state of the dielectron in $(H_2O)_{256}^-$ at 300 K.

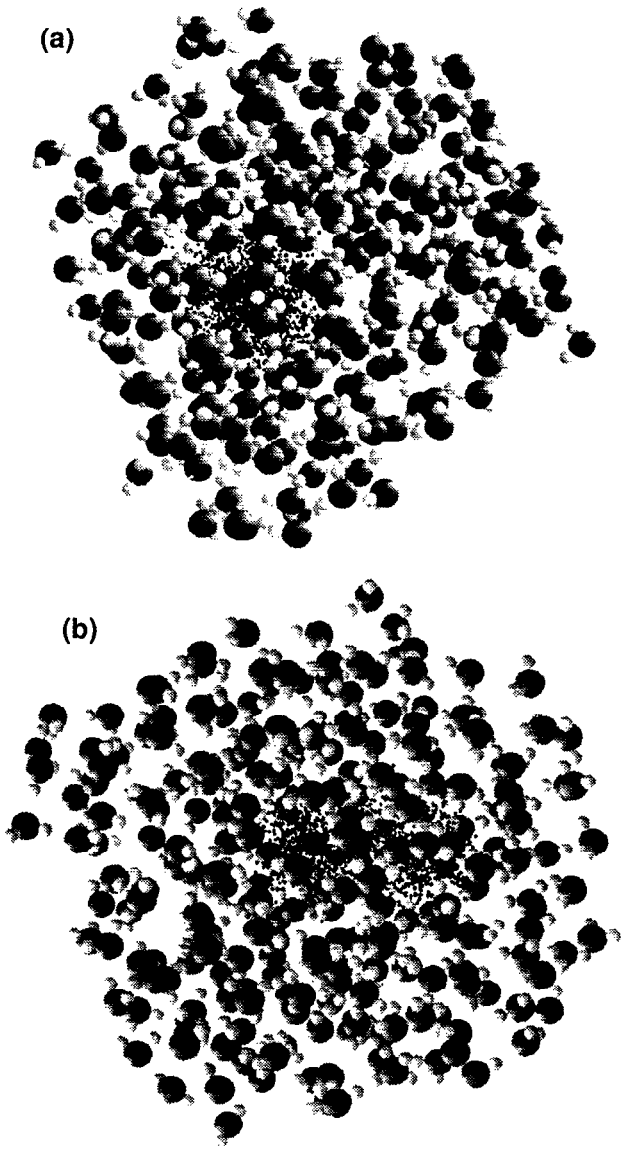

FIG. 4. Atomic configurations of the water molecules and electron distributions of the compact [e_{2c}, in (a)] and dumbbell-shaped [e_{2d}, in (b)] states of the internally localized dielectron in $(H_2O)_{256}^-$ at 300 K. Large dark spheres and small light ones correspond to oxygens and hydrogens, respectively. The electronic distribution is represented by the black dots.

The fluctuations between the two dielectron states along the system trajectory are exhibited in Fig. 7(a) where $\Delta\zeta = (\int d^3r\{p(\mathbf{r})/[\rho_\uparrow(\mathbf{r}) + \rho_\downarrow(\mathbf{r})]\}^2)^{1/2}$ (the integration is over the spatial grid) is shown vs the number of integration time steps in a segment of the simulation. As seen in this segment the system converted first from an e_{2d} to an e_{2c} state ($n_{\text{step}} \sim 2250$) which transformed back to the e_{2d} state. Later ($n_{\text{step}} \sim 4250$) an $e_{2d} \rightarrow e_{2c}$ transformation occurred followed by several short-lived fluctuations toward the e_{2d} state. In this context we note that we observed such behavior both in simulations employing the original or modified pseudopotentials, and regardless of the starting configuration of the dielectron.[21]

As observed from Table I for the e_{2c} and e_{2d} states, as well as for the intermediate short-lived transition state e_{2i} (obtained for each state via averaging the properties of the system over the corresponding segments of the simulation), the energetic properties of the system in these states are quite similar [corresponding results for $(H_2O)_{256}^-$ calculated with the unmodified pseudopotential are given in Appendix C].

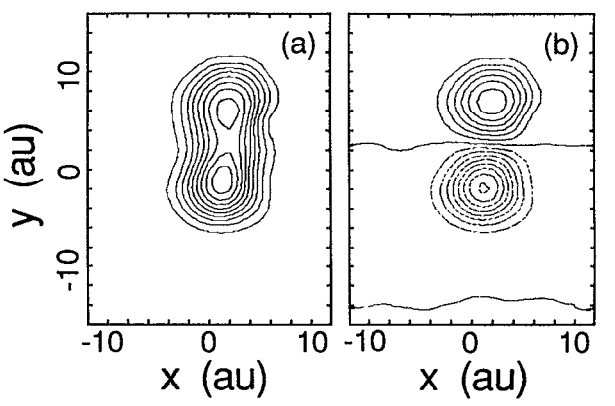

FIG. 6. Contours of electronic density (a) and spin-polarization function $p(\mathbf{r})$ (b) for the e_{2d} state of the dielectron in $(H_2O)_{256}^-$ at 300 K. The maximum density at the foci of the electronic density in (a) is 0.0049 e/a_0^3. The maxima of the $p(\mathbf{r})$ contours in (b) are 0.0034 e/a_0^3 (upper contours) and -0.0041 e/a_0^3 (lower contours).

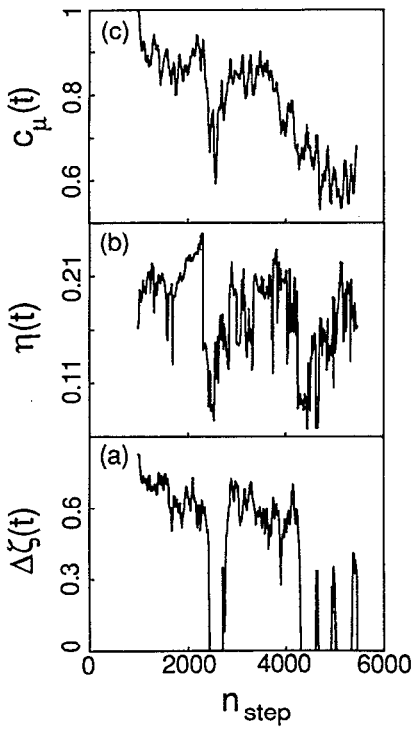

FIG. 7. Spin-polarization $\Delta\zeta$ (a), and order parameters η and C_μ (b), (c) for a segment of the simulation of a dielectron in $(H_2O)_{256}^-$ at 300 K, plotted vs the number of integration time steps (n_{step}). Note transitions between the dielectron states associated with sharp variations in $\Delta\zeta$ and the order parameters, indicating structural and molecular orientation transformations accompanying the transitions between the e_{2c} and e_{2d} states.

The electronic distributions in the two states of the dielectron can be characterized by their radii of gyration whose components in the e_{2c} state are $(R_{gx},R_{gy},R_{gz}) = (2.8\ [0.23]\ a_0,\ 2.7\ [0.35]\ a_0,\ 3.0\ [0.35]\ a_0)$ yielding an average value $R_g \simeq 4.9\ a_0$, and in the e_{2d} state (2.6 [0.2] a_0, 4.3 [0.5] a_0, 2.3 [0.2] a_0), where the values in square brackets are the estimated calculational uncertainties. These values may be compared with the average radius of gyration of the nearly spherical distribution for a single excess electron in $(H_2O)_{256}^-$, where $R_g = 3.75\ a_0$.

The transition between the e_{2c} and e_{2d} states of the dielectron are accompanied by structural variations of the surrounding water molecules. To illustrate these configurational variations we define the following structural order parameters:

$$\text{(a)}\quad \eta(t) = \frac{c(t) - \frac{1}{2}[a(t)+b(t)]}{c(t) + \frac{1}{2}[a(t)+b(t)]}, \tag{7}$$

where $a(t)$, $b(t)$, and $c(t)$ are the magnitudes, in increasing order, of the principal axes of the moments of inertia tensor of the distribution of water molecules surrounding the dielectron (in our calculations these were computed for the oxygens of the ten water molecules closest to the centroid of the dielectron distribution, i.e., $R_{e_2-O} \lesssim 8.5\ a_0$). (b) The molecular dipole correlation function

$$C_\mu(t) = \frac{\langle \boldsymbol{\mu}(0)\cdot\boldsymbol{\mu}(t)\rangle}{\langle \boldsymbol{\mu}(0)\cdot\boldsymbol{\mu}(0)\rangle}, \tag{8}$$

where the angular brackets denote averaging over the closest ten water molecules as described above.

These order parameters plotted vs n_{step} are shown in Fig. 7(b) and 7(c). Comparison with the variations in $\Delta\zeta(t)$ [Fig. 7(a)] shows characteristic variations in these parameters coincident with the transitions between the two states of the dielectron; the magnitude of $\eta(t)$ achieves a significantly smaller value for the e_{2c} state corresponding to a nearly spherical cavity, and the variations in $C_\mu(t)$ indicate molecular orientational transformations accompanying the transitions between the dielectron states.[22]

Further characterization of the dielectron states is provided by the configurations and atomic distribution contours for the e_{2c} and e_{2d} states shown in Figs. 8 and 9, respectively. These figures provide added evidence for the spherical-like and elongated ellipsoidal shapes of the dielectron distributions and solvation cavities in the two states as well as indicating the preferential orientational ordering of the water molecules surrounding the dielectron.

The solvation shell structure of the dielectron in

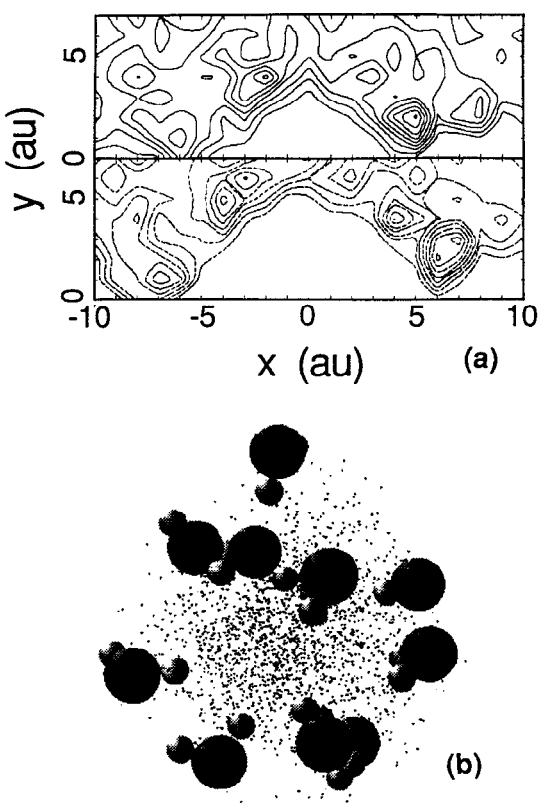

FIG. 8. (a) Contours of atomic distributions in the xy plane for the e_{2c} dielectron state in $(H_2O)_{256}^-$ at 300 K. Top contours are for the hydrogens and the bottom ones for the oxygens of H_2O molecules in the vicinity of the dielectron. Only the upper hemisphere of the e_{2c} cavity is shown (averaged around the x axis). (b) Atomic configurations of the water molecules (large dark spheres and small light ones corresponding to oxygens and hydrogens, respectively) and dielectron distribution (represented by black dots) corresponding to the contours shown in (a).

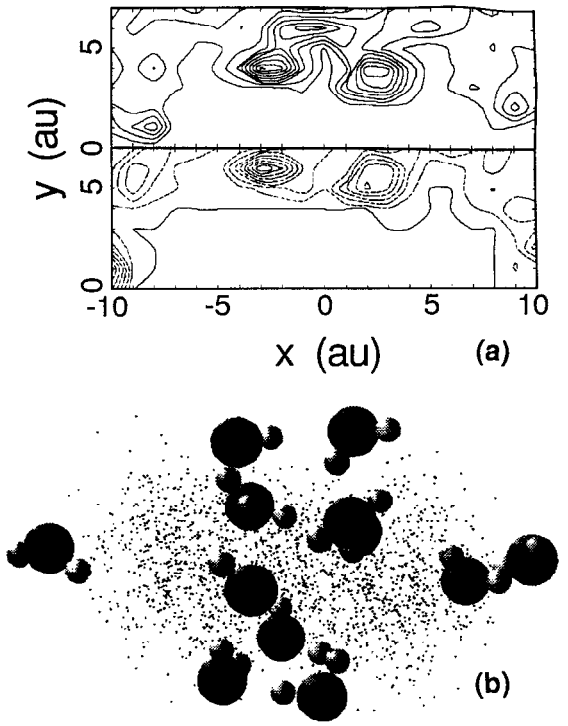

FIG. 9. Same as Fig. 8 but for the e_{2d} state of the dielectron in $(H_2O)_{256}^{-2}$ at 300 K. The vector connecting the two electron-density maxima of the elongated e_{2d} state is rotated to lie along the x axis.

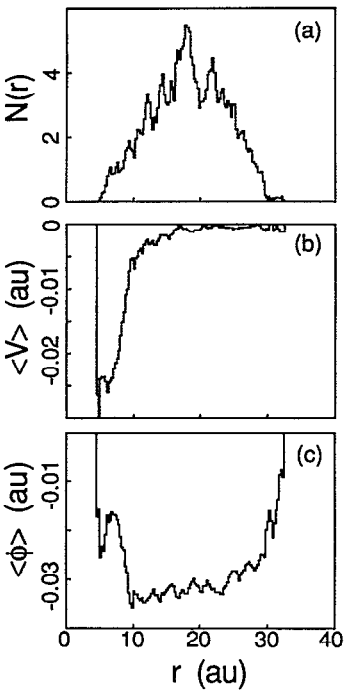

FIG. 10. Radial plots vs r of the average number of oxygens [$N(r)$, in (a)], of the electron–water interaction [$\langle V \rangle$, in (b)], and the molecular interaction energy [$\langle \phi \rangle$, in (c)] in a sphere of radius r about the centroid of the e_{2c} distribution in $(H_2O)_{256}^{-2}$ at 300 K. Energy in units of a.u. (1 a.u. = 27.21 eV) and distance in units of the Bohr radius (1 a.u. = 1 a_0).

$(H_2O)_{256}^{-2}$ is exhibited in Fig. 10(a) for the e_{2c} state where the average number of oxygens [$N(r)$] in a sphere of radius r about the centroid of the dielectron distributions is plotted vs r. Additionally, radial distributions for the electron–water interaction and molecular interaction potential energies are shown in Figs. 10(b) and 10(c), respectively. The molecular radial distribution for the e_{2c} state in $(H_2O)_{256}^{-2}$ is more structured than the one for the single excess electron [see Appendix B, Fig. 15(a)], with the structure in the cluster induced by the excess dielectron extending to molecular solvation shells further away from the centroid of the e_{2c} distribution than is the case in $(H_2O)_{256}^{-1}$. This correlates with the much stronger and somewhat longer-range interaction between the electrons and the water molecules in $(H_2O)_{256}^{-2}$ as compared with the single-electron system [compare Figs. 10(b) and 15(b)], and is also reflected in the radial molecular interaction energy [compare Figs. 10(c) and 15(c)] where the influence of the dielectron is seen to effect the water structure over a relatively large range. From these plots we assign the first three solvation shells of the dielectron as $(0, 8\,a_0)$, $(8\,a_0, 10\,a_0)$, and $(10\,a_0, 15\,a_0)$ containing on the average ~ 8.9, 11.7, and 54.2 water molecules, respectively. For the $(H_2O)_{256}^{-1}$ system the corresponding solvation shells are defined as $(0, 7\,a_0)$, $(7\,a_0, 10.5\,a_0)$, and $(10.5\,a_0, 14.5\,a_0)$, containing 6.2, 18.7, and 44.2 water molecules, respectively (see Appendix B). While in the dielectron case the differentiation between shells is somewhat ambiguous (though the induced molecular structure is well defined), it is obvious that the number of molecules in the first (proximal) solvation region is larger in $(H_2O)_{256}^{-2}$ than in the singly charged cluster.

Analysis of the solvation shell structure for the e_{2d} state is complicated by the lack of approximate spherical symmetry. However, radial plots as those shown in Fig. 10, neglecting the ellipsoidal shape of the cavity, yield solvation shell radii of $(0, 8\,a_0)$, $(8\,a_0, 11.5\,a_0)$, and $(11.5\,a_0, 14.5\,a_0)$ containing an average number of 8.1, 11.5, and 35 water molecules, with relatively small variations (10%–20%) when using ellipsoidal coordinates.

To conclude this section we use the above solvation-shell radii definitions to explore the degree of orientational molecular order in the shells for the e_{2c} state. The orientational distributions of the molecular O–H bonds, in the first three solvation shells, with the centroid of the dielectron distribution taken as the origin, are shown in Fig. 11 (θ is the angle between $\mathbf{r}_{e_2\text{–O}}$, the vector connecting the molecular oxygen and the centroid of the dielectron, and the O–H bonds). As seen, molecules in the first solvation shell are strongly preferentially oriented with one of the O–H bonds of each molecule pointing toward the center of the dielectron distribution (for perfect orientational order $\cos\theta_{e_2\text{–OH}_{(1)}} = 1$, while for the other bond of the molecule $\cos\theta_{e_2\text{–OH}_{(2)}} = -0.25$). Pronounced OH bond-orientational preferrence is found also in the second, and to a lesser extent in the third, solvation shells. Comparison with the $(H_2O)_{256}^{-1}$ case (see Fig. 16 in Appendix B) illustrates the stronger orientational ordering induced by the localized die-

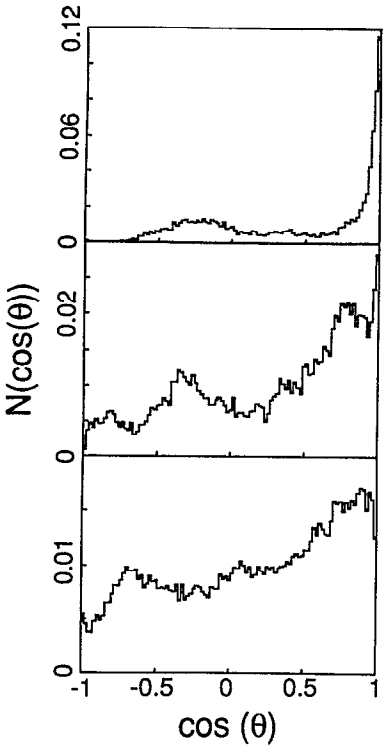

FIG. 11. Orientational distributions of the molecular O–H bonds in the first three solvation shells (first shell at the top) for the e_{2c} state in $(H_2O)_{256}^{-2}$ at 300 K.

lectrons and the more extended range of the effect, corraborating our previous conclusions.

IV. SUMMARY

In this study we investigated, using modern simulation methods of coupled classical-quantum molecular dynamics the equilibrium energetics, structure, and stability of a dielectron solvated in an internal cavity in water clusters $(H_2O)_n^{-2}$, $n = 64$, 128, and 256, and in bulk water, at 300 K. As noted before, the issue of the existence and properties of such a solvated species in water is of conceptual interest since it forms an analog of the well-known F' center in ionic crystals and is an important electron localization mode in disordered solids and liquids (bipolaron). In addition, in the context of clusters a dielectronic state extends our notion of bipolarons to finite systems. Furthermore, physical characterization of the dielectron state in water may be of relevance and importance for the analysis of post-radiative processes such as excess electron recombination and of chemical reactions (such as H_2 production) whose mechanisms are likely to involve concerted action by two proximal electrons. In this context we reiterate that the expected reactivity of the dielectron state in water may complicate experimental probing of its properties. Nevertheless, it is hoped that the application of refined fast spectroscopies would allow such future studies.

Among the various possible solvation modes of two excess electrons in a water cluster, we focused in this study on the one where the two electrons are internally localized, proximal to each other. The main results of our study may be summarized as follows.

(a) An internally localized dielectron is unstable in a water cluster containing 64 molecules, and is marginally stable (if at all) in $(H_2O)_{128}^{-2}$.

(b) An internally localized ground-state spin-paired (i.e., ^1S) dielectron in $(H_2O)_{256}^{-2}$ (Table I and Fig. 2(a); see also Table IV in Appendix C) is energetically stable (though perhaps of a short lifetime due to possible reactions with the water medium). In addition, extrapolation to the bulk water case yields a ground-state dielectron adiabatic binding energy of ~ -6.5 eV (or ~ -4.1 eV using another method of estimation, see Sec. II A) when using the modified electron–water pseudopotential. A lower value, i.e., more binding, is obtained when using the unmodified pseudopotential. These values may be compared with that calculated via a semicontinuum model[13] where, assuming a value of -1.0 eV for the conduction-band edge in water (V_0 in Table II in Ref. 13), a dielectron adiabatic binding energy of ~ -7.9 eV was obtained. Note, however, that the structural properties which were obtained via the semicontinuum model[13] differ from those found in our microscopic simulations (see Sec. III).

(c) The adiabatic dissociation energy of the ground-state electron in bulk water into two separated hydrated electrons is calculated to be ~ 1.65 eV, or 0.82 eV using another method of estimation (compare to 2.4 eV in Ref. 13), and the first vertical and adiabatic ionization potentials of $(H_2O)_{256}^{-2}$ (i.e., $(H_2O)_{256}^{-2} \rightarrow [(H_2O)_{256}^{-1}]_2 + e^-$ and $(H_2O)_{256}^{-2} \rightarrow (H_2O)_{256}^{-1} + e^-$, respectively) are calculated to be ~ 1.2 eV and 0.2 eV, respectively. The first vertical ionization potential of a dielectron in bulk water is estimated to be ~ 3.6 eV.

(d) The vertical ionization energy of the ground-state dielectron in the 256 water molecule cluster (i.e., $(H_2O)_{256}^{-2} \rightarrow [(H_2O)_{256}]_2 + 2e^-$) is ~ 7.5 eV, and the corresponding ionization energy of the dielectron in bulk water is estimated to be ~ 12.5 eV.

(e) The main attractive contribution to the total energy of the dielectron is from the long-range interaction of the electrons with the water molecules, which together with the exchange contribution is of larger magnitude (but of opposite sign) in $(H_2O)_{256}^{-2}$ and in bulk water than the repulsion originating from the interelectronic Hartree interaction, the electronic kinetic energy, and the cluster molecular reorganization energy. The reorganization energy associated with the formation of the solvation cavity of the dielectron is significantly larger than that associated with the hydration of a single excess electron.

(f) The internally equilibrium solvated dielectron in $(H_2O)_{256}^{-2}$ fluctuates between a compact state of approximate spherical symmetry (e_{2c}) and an elongated ellipsoidal dumbbell-shaped state (e_{2d}). In both of these ground-state configurations the dielectron is in a spin-paired ^1S state. In the e_{2d} state the maxima of the electronic distribution are separated by $\sim 8\,a_0$. The dielectron transitions between the two approximately degenerate states are accompanied by molecular solvation-cavity shape fluctuations and orientational transformations of the surrounding water molecules.[22]

(g) The radius of gyration, R_g, of the dielectron distribution in $(H_2O)_{256}^{-2}$ in the e_{2c} state is $\sim 4.9\,a_0$, compared to a smaller value for a solvated single excess electron where $R_g \sim 3.75\,a_0$.

(h) The solvation cavity for the dielectron in the e_{2c} state is slightly larger than that for a single solvated electron. The dielectron induces a solvation-shell structure in the surrounding water medium, with the first solvation shell of radius $\sim 8\,a_0$ (in the e_{2c} state) containing ~ 9 molecules, (the values for the e_{2d} state vary by about 10%–20%). This may be compared with the somewhat smaller first solvation-shell radius for a single solvated excess electron ($\sim 7\,a_0$), containing a significantly smaller number of water molecules (~ 6).

(i) Similar to the single solvated electron case the dielectron induces orientational order in the surrounding water medium, with O–H bonds of the water molecules preferentially oriented toward the centroid of the dielectron distribution. The degree of orientational order and its range are larger for the dielectron case.

(j) Certain aspects of the energetics and structure of a dielectron in water in comparison to the properties of a single hydrated electron correlate with the properties of a solvated negatively charged divalent ion relative to those of a solvated singly charged anion. However, the aforementioned fluctuations between the two ground-state configurations of the hydrated dielectron [see (f) above] are a unique property of the quantum solvated species.[22]

ACKNOWLEDGMENTS

We gratefully acknowledge useful conversations with Professor Abraham Nitzan concerning the electron–water interactions. This research is supported by the U.S. Department of Energy (DOE) under Grant No. FG05-86ER45234. H.-P. K gratefully acknowledges partial support by the Foundation of Neste Corporation, the Wihuri Foundation, and the Finnish Academy of Sciences. Most calculations were performed at the Florida State and Pittsburgh Supercomputer Centers, and in part at the National Energy Research Supercomputer Center, Livermore, California, through a computer grant by the DOE.

APPENDIX A

In this appendix equilibrium results for neutral water clusters, $(H_2O)_n$, $n = 64$, 128, and 256, at 300 K, obtained via simulations using the RWK2-M water potentials, are given in Table II.

In the molecular-dynamics (MD) simulations the equations of motions were integrated using Gear's fifth-order predictor–corrector algorithm with an integration time step $\Delta t = 0.25$ fs. Averages were performed, after prolonged equilibration (with infrequent thermalization using the stochastic collision method), over runs of $1.6\times 10^5 \Delta t$ for $n = 64$, and $10^5 \Delta t$ for $n = 128$ and 256. The estimated errors (standard deviation of 10 subaverages) are given in square brackets.

TABLE II. Average intra-($\langle \Phi^{(1)} \rangle$) and inter-($\langle \Phi^{(2)} \rangle$) molecular potential energies, and total potential energies, for neutral $(H_2O)_n$ clusters at $T = 300$ K. Energies in a.u. units (1 a.u. = 27.21 eV).

n	$\langle \Phi^{(1)} \rangle$	$\langle \Phi^{(2)} \rangle$	$\langle \Phi \rangle$
64	0.1450	−0.9279	−0.7829 [0.010]
128	0.2985	−1.9963	−1.6977 [0.014]
256	0.6111	−4.1944	−3.5832 [0.027]

APPENDIX B

In this appendix we describe the energetics and structure of single excess electrons internally localized in $(H_2O)_n^-$ ($n \geqslant 64$) clusters, calculated at 300 K via the ground-state dynamics method [GSD, see Refs. 4(c) and 5(b)] with the modified electron–water interaction pseudopotential (see Sec. II). Since the properties of excess electrons in water clusters of variable sizes have been discussed by us previously, we limit ourself here to a brief discussion of the main characteristics of $(H_2O)_n^-$ which can be used to compare with the dielectron results given in Sec. III.

Prior to presentation of our results we show in Fig. 12 equipotential contours of the modified pseudopotential [Fig. 12(a)] [compare with Fig. 1 in Ref. 3(a)] and difference contours between the modified and original pseudopotential [Fig. 12(b)]. In addition, we show in Fig. 13 comparative linear plots of the two electron–water pseudopotentials along one of the O–H bonds of the molecule. We observe that the main effect of the modification is confined to the vicinity of the molecule where the modified pseudopotential is more binding (due to the increased relative contribution of the attractive exchange-correlation term).

The energetics of internally localized states is exhibited in Table III and in Fig. 14 where the vertical and adiabatic energies are plotted vs $n^{-1/3}$ [for $(H_2O)_n^-$ with $n \leqslant 32$ the excess electron was found to localize in a surfacelike state, and since our focus in this paper is on internally solvated electrons only data for such systems is given]. As may be

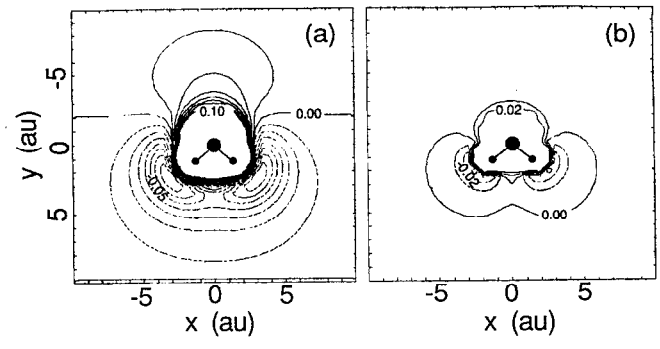

FIG. 12. (a) Equipotential contours of the modified electron–water pseudopotential (see Sec. II) in the plane of the H_2O molecule (shown in the middle). (b) Difference contours between the modified and original electron–water pseudopotentials.

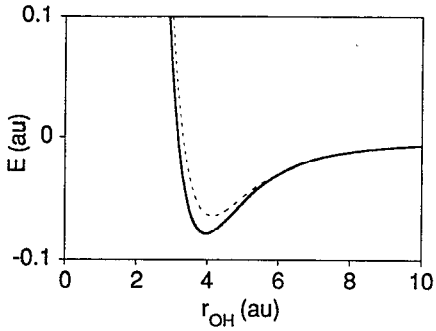

FIG. 13. Variation of the modified (solid line) and original (dashed line) electron–water pseudopotentials plotted vs distance along one of the O–H bonds. Energy in a.u. units (1 a.u. = 27.21 eV), and distance in Bohr radius (a_0).

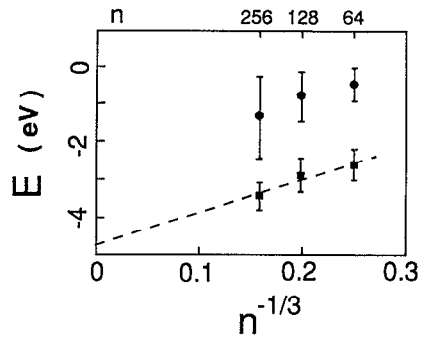

FIG. 14. Vertical (solid squares) and adiabatic (solid circles) binding energies of a single excess electron in $(H_2O)_n^-$, $n = 64$, 128, and 256, at 300 K, plotted vs $n^{-1/3}$. The modified electron–water pseudopotential was used in the calculations. Energy in eV.

ascertained by comparing these results with those obtained by us previously,[3(b),4(c),5(b),6] and with recently published photoelectron data,[4(b)] the correspondence between the binding energies for $(H_2O)_n^-$ ($n \geqslant 64$) calculated with the modified pseudopotential and those deduced from experiments is improved. While the bulk intercept of the VBE's (VBE^∞, i.e., $n^{-1/3} \to 0$ in Fig. 14) is still lower than the experimentally and theoretically estimated ones [$-4 \leqslant VBE^\infty \leqslant -3.2$ eV; see Ref. 4(b), and references therein], we note that its magnitude is decreased compared to our previous analysis[3(b),4(c),5(b),6] (furthermore in view of the calculational error estimates the value indicated by the extrapolation of the dashed line in Fig. 14 may be regarded as a lower bound of the bulk value). Similarly, extrapolation of the ABE's to the bulk limit, and consideration of the large calculational uncertainties (see Fig. 14), yields an estimate in reasonable correspondence with the experimentally estimated heat of hydration of an electron in bulk water [$\Delta H(e_{aq}^-) \approx -1.7$ eV; see Ref. 19].

Since the dielectron calculations were performed using the LSD method, we have performed for the single-excess-electron systems comparative LSD and GSD calculations which confirmed that the results obtained by the two methods differed by at most 2% (i.e., an almost complete cancellation between the Hartree and exchange-correlation contributions in the LSD calculations), justifying the use of the results given in Table III in analyzing the stability of the dielectron (see Sec. III).

The solvation structure in $(H_2O)_{256}^-$ is portrayed in the radial plot of $N(r)$ shown in Fig. 15(a), where the number of oxygens in a sphere of radius r about the centroid of the excess electron is given vs r. From this data the first three solvation-shell radii are determined: (0, 7 a_0), (7 a_0, 10.5 a_0), and (10.5 a_0, 14.5 a_0), containing an average number of 6.2, 18.7, and 44.2 water molecules, respectively (in good correspondence with our previous results). The radial plots of the electron–water interaction ($\langle V \rangle$) and molecular interaction energies ($\langle \phi \rangle$) shown in Figs. 15(b) and 15(c), indicate the finite range of $\langle V \rangle$ and the effect of the solvated electron on the water structure (i.e., molecular reorganization mainly due to the solvation cavity formation). As noted in Sec. III the induced effect of the dielectron on the solvent molecules extends over a larger range than that of the single solvated electron. This is also evident from comparison of

TABLE III. Energetics of single excess electron internally localized in an $(H_2O)_n^-$ cluster at 300 K using the modified electron–molecule pseudopotentials. $\langle \phi_1 \rangle_1$, $\langle \phi_2 \rangle_1$, and $\langle \phi \rangle_1$ are, respectively, the intra- and intermolecular contributions of the cluster, and their sum to the molecular potential energy. $\langle V \rangle_1$ and $\langle K \rangle_1$ are the potential and kinetic energies of the excess electron, respectively, and $VBE_1 = \langle V \rangle_1 + \langle K \rangle_1$ is the vertical binding energy. E_{c1} is the cluster reorganization energy and $ABE_1 = VBE_1 + E_{c1}$ is the adiabatic binding energy. R_g is the radius of gyration of the excess electron distribution. Calculational uncertainty estimates are given in square brackets. Energies are in units of a.u., and R_g in units of Bohr radius (a_0).

	$\langle \phi_1 \rangle_1$	$\langle \phi_2 \rangle_1$	$\langle \phi \rangle_1$	$\langle V \rangle_1$	$\langle K \rangle_1$	E_{c1}	VBE_1	ABE_1	R_g
64	0.1438	−0.8480	−0.7042	−0.1916	0.0955	0.0787	−0.0961 [0.0153]	−0.0174	3.8
128	0.2886	−1.9090	−1.6203	−0.1986	0.0918	0.0774	−0.1069 [0.016]	−0.0295	3.8
256	0.6002	−4.1070	−3.5068	−0.2228	0.0966	0.0764	−0.1262 [0.0127]	−0.0498	3.75

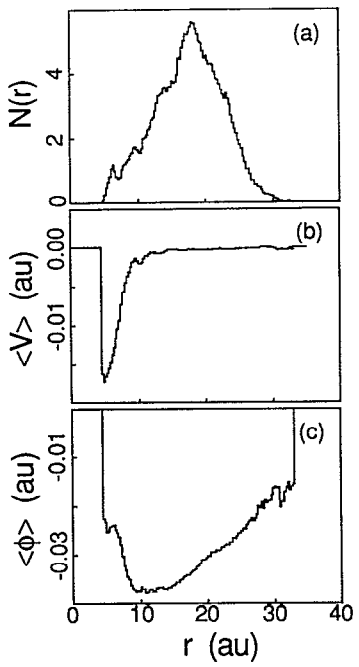

FIG. 15. Radial plots vs r of the average number of oxygens [$N(r)$, in (a)], the electron–water interaction [$\langle V \rangle$, in (b)], and the molecular interaction energy [$\langle \phi \rangle$, in (c)] in a sphere of radius r about the centroid of the excess electron distribution.

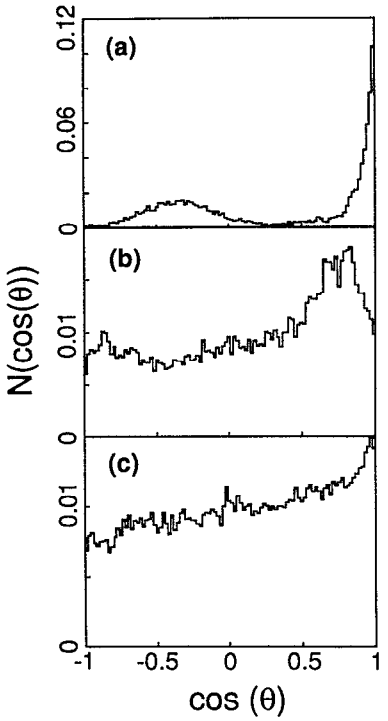

FIG. 16. Orientational distributions of the molecular O–H bonds in the first three solvation shells [(a), (b), and (c)] for a single electron localized in $(H_2O)_{256}^-$ at 300 K.

Fig. 10 with the orientational distributions of the molecular O–H bonds in the first three solvation shells in $(H_2O)_{256}^-$, as shown in Fig. 16.

Finally, we comment that the general characteristics of the excited states and spectral properties of $(H_2O)_n^-$ clusters calculated with the modified pseudopotential are found to be similar to those discussed by us previously.[6] We note, however, that both the 1s-like ground electronic state and p-like excited states of the internally localized electrons are shifted in the present calculations to higher values than in the previous ones (resulting in smaller magnitudes of the VBE's). However the amount by which the ground and excited states are shifted to the red are not the same. This results (after weighing the transition energies by the corresponding dipole matrix elements) in simulated spectra with maxima for $n = 64$, 128, and 256 at $\sim$2.1, 2.3, and 2.55 eV, respectively, with the spectral line shapes characterized by a width of $\sim$1 eV (these peak positions are somewhat higher than the corresponding ones calculated by us previously[6]).

TABLE IV. Energetics of a dielectron internally localized in an $(H_2O)_{256}^-$ cluster, at 300 K, calculated with the unmodified electron–water pseudopotential. $\langle \phi_1 \rangle_2$, $\langle \phi_2 \rangle_2$, and $\langle \phi \rangle_2$ are the intra-, inter-, and total potential energies of the water molecules. $\langle V \rangle_2$, $\langle K \rangle_2$, $\langle E_{xc} \rangle_2$, and $\langle E_H \rangle_2$ are the contributions of the electron–water interaction, electronic kinetic energy, exchange-correlation term, and Hartree energy, respectively, to the total dielectron energy. VBE_2 is the vertical binding energy of the dielectron (i.e., the sum of the aforementioned contributions); E_{c2} is the cluster molecular reorganization energy, and ABE_2 is the adiabatic binding energy, $ABE_2 = VBE_2 + E_{c2}$. Results for the e_{2c}, e_{2d}, and e_{2i} dielectron states were averaged over $4\times10^3\Delta t$, $5\times10^3\Delta t$, and $5\times10^2\Delta t$, respectively. The average properties of the dielectron are given in the first row. Uncertainty estimates are given in square brackets, and energies in a.u. units (1 a.u. = 27.21 eV).

	$\langle \phi_1 \rangle_2$	$\langle \phi_2 \rangle_2$	$\langle \phi \rangle_2$	$\langle V \rangle_2$	$\langle K \rangle_2$	$\langle E_{xc} \rangle$	$\langle E_H \rangle_2$	E_{c2}	VBE_2	ABE_2
average	0.6175	−4.0155	−3.3980 [0.030]	−0.5976	0.1489	0.2280	0.3725	0.185	−0.304 [0.023]	−0.119
e_{2c}	0.6154	−3.9979	−3.3825	−0.6000	0.1355	0.2227	0.3840	0.20	−0.303 [0.02]	−0.1025
e_{2d}	0.6194	−4.0274	−3.4080	−0.5978	0.1613	0.2335	0.3634	0.175	−0.307 [0.025]	−0.1314
e_{2i}	0.6161	−4.0403	−3.4242	−0.5780	0.1378	0.2183	0.3683	0.159	−0.290 [0.015]	−0.1312

In this context we note that the peak position for the absorption spectrum of the surface state in $(H_2O)_{32}^{-1}$ calculated with the modified pseudopotential is at ~ 0.9 eV (in agreement with our previous calculations[6]), thus confirming our earlier prediction[6] that the absorption bands associated with surface, or surfacelike, states peak at energies lower than those associated with interior excess electron states.

APPENDIX C

In this appendix we give in Table IV results for the energetics of a dielectron internally localized in an $(H_2O)_{256}^{-2}$ cluster, using the unmodified electron–water pseudopotential. The structural properties (e.g., solvation-shell structure and molecular preferential orientations) are similar to those shown in Sec. III for calculations using the modified pseudopotential.

[1] E. J. Hart and J. W. Boag, J. Am. Chem. Soc. **84**, 4090 (1962).

[2] W. Weyl, Ann. Phys. (Leipzig) **197**, 601 (1963).

[3] For an extensive list of references, see (a) R. N. Barnett, U. Landman, C. L. Cleveland, and J. Jortner, J. Chem. Phys. **88**, 4421 (1988); (b) **88**, 4429 (1988).

[4] See reviews and references in (a) R. N. Barnett, U. Landman, G. Rajagopal, and A. Nitzan, Isr. J. Chem. **30**, 85 (1990); (b) J. V. Coe, G. H. Lee, J. G. Eaton, S. T. Arnold, H. W. Sarkas, K. H. Bowen, C. Ludewigt, H. Haberland, and D. R. Worsnop, J. Chem. Phys. **92**, 3980 (1990); (c) R. N. Barnett, U. Landman, and A. Nitzan, *ibid.* **89**, 2242 (1988).

[5] (a) R. N. Barnett, U. Landman, and A. Nitzan, J. Chem. Phys. **90**, 4413 (1989); (b) *ibid.* **91**, 5567 (1989); Phys. Rev. Lett. **62**, 106 (1989); (c) E. Neria, A. Nitzan, R. N. Barnett, and U. Landman, *ibid.* **67**, 1011 (1991).

[6] R. N. Barnett, U. Landman, G. Makov, and A. Nitzan, J. Chem. Phys. **93**, 6226 (1990).

[7] See review in P. J. Rossky and J. Schnitker, J. Phys. Chem. **92**, 4277 (1988).

[8] F. A. Webster, P. J. Rossky, and R. A. Friesner, Comput. Phys. Commun. **63**, 494 (1991); Phys. Rev. Lett. **66**, 3172 (1991).

[9] A. Migus, Y. Gandel, J. L. Martin, and A. Antonetti, Phys. Rev. Lett. **58**, 1529 (1987); F. H. Long, H. Lu, and K. B. Eisenthal, *ibid.* **64**, 1469 (1990).

[10] W. B. Fowler, *Physics of Color Centers* (Academic, New York, 1968).

[11] See review by W. W. Warren, Jr., in *The Metallic and Non Metallic States of Matter*, edited by P. P. Edwards and C. N. Rao (Taylor and Francis, London, 1985); A. Selloni, E. S. Fois, M. Parrinello, and R. Car, Phys. Scr. **T25**, 261 (1989).

[12] See G. Rajagopal, R. N. Barnett, and U. Landman, Phys. Rev. Lett. **67**, 727 (1991), and references therein.

[13] See D.-F. Feng, K. Fenki, and L. Kevan, J. Chem. Phys. **58**, 3281 (1973), and references therein.

[14] See N. R. Kestner in *Electron-Solvent and Anion-Solvent Interactions*, edited by L. Kevan and B. C. Webster (Elsevier, Amsterdam, 1976), p. 1, and references therein.

[15] J. R. Reimers, R. O. Watts, and M. L. Klein, Chem. Phys. **64**, 95 (1982); J. R. Reimers and R. O. Watts, *ibid.* **85**, 83 (1984); see also Ref. 3(a).

[16] R. N. Barnett and U. Landman (unpublished).

[17] K. H. Bowen (unpublished).

[18] R. N. Barnett, U. Landman, and J. Jortner, Chem. Phys. Lett. **145**, 382 (1988).

[19] G. Lepoutre and J. Jortner, J. Phys. Chem. **76**, 682 (1972).

[20] R. N. Barnett and U. Landman (unpublished).

[21] In addition to starting the dielectron simulations from cluster configurations obtained via single-excess-electron calculations, other starting configurations were used. For example, in some dielectron simulations we have used as initial configurations dumbbell-shaped internal cavities obtained via simulations of two neighboring negative classical point charges, interacting each with the water molecules via a repulsive potential adjusted to yield a solvation cavity of radius comparable to that of a solvated electron in the water cluster. In all cases for the $(H_2O)_{256}^{-2}$ cluster, the solvated equilibrium dielectron exhibited transitions between the e_{2c} and e_{2d} states.

[22] The transitions between the spherically compact (e_{2c}) state and the dumbbell-shaped (e_{2d}) state of the dielectron, and the molecular reorganization associated with them, suggest a polaronic diffusion mechanism of a dielectron in water involving such transitions.